

## Switching azobenzene derivatives on Au(111) analyzed by advanced computer vision methods

Robert di Vora<sup>a</sup>, Matthew James Timm<sup>b</sup>, Alexander Eber<sup>a</sup>, Emily Hruska<sup>a</sup>, Stefan Hecht<sup>c</sup>, Leonhard Grill<sup>b,\*</sup>, Birgitta Bernhardt<sup>a,\*\*</sup>

<sup>a</sup> Graz University of Technology, Experimental Physics, Coherent Sensing Group, Petersgasse 16, 8010 Graz, Austria

<sup>b</sup> University of Graz, Physical Chemistry Division, Heinrichstrasse 28, 8010 Graz, Austria

<sup>c</sup> Humboldt-University of Berlin, Department of Chemistry and Center for the Science of Materials Berlin, Zum Großen Windkanal 2, Berlin, Germany

### ARTICLE INFO

#### Keywords:

Laser STM  
Computer vision  
Azobenzene  
Isomerization statistics  
mTBA  
trans-cis  
optical switch  
molecular switch

### ABSTRACT

The light induced *trans-cis* isomerization of azobenzene allows studying and controlling the properties of photosensitive materials. Promising applications include optical switching, data storage, and light-driven nanomechanical devices. Understanding switching in molecular assemblies is essential to scale these photoinduced mechanisms for practical applications. In this study, we analyze the switching behavior of single azobenzene derivatives in large assemblies ( $n \gg 10^3$ ) with advanced computer vision techniques. This approach enables us to detect subtle variations in switching yields among densely packed, similarly oriented molecules. Our findings provide new insights into the switching of molecular assemblies.

### 1. Introduction

The light-induced *trans-cis* isomerization of azobenzene and its derivatives is of great scientific and technological interest [1–10]. This behavior might be harnessed to realize controllable, molecule-sized switches that convert optical energy to mechanical work [11–14]. Such photo-switching molecules have applications ranging from pharmaceuticals [7,8] to nano-scale sensing [15,16] or information and energy storage [17–20]. The photo-switching properties of such compounds in solution are well documented [21–28]. Additionally, their properties following adsorption upon insulating [29,30] and conductive surfaces [31–40] and at the solid-liquid interface [41] have been the subject of significant investigation using scanning probe microscopy and density functional theory (DFT). In particular, the adsorption characteristics and photo-switching mechanisms for azobenzene derivatives adsorbed upon Au(111) have been a major topic of study using scanning tunneling microscopy (STM) [42–60], two-photon photoemission (2PPES) [61–64] and X-ray absorption spectroscopy (XAS) [65–67]. Such studies have demonstrated how external stimuli such as tunnelling electrons [44,50,60,68] electric field [47,58,59], heat [61,62,64], or

light [45,52–56,61–63,69] can be used to isomerize, or “switch”, azobenzene molecules between the *cis* and *trans* isomers [44,47,50,52,56,58,60,68] or to collectively control the *cis* or *trans* state of groups of molecules within self-assembled monolayers or states characterized by higher mobility of the molecules [45,53].

A compound that has received great attention is 3,3',5,5'-tetra-*tert*-butylazobenzene (mTBA) [36,37,61,62,69–71]. This switching behaviour of this compound at a surface has been studied at the single-molecule level by STM and DFT [36,37,54–60] at sub-monolayer coverage ( $< 0.1$  ML), as well as at near monolayer coverage (0.9 ML) by the ensemble-averaging techniques of 2PPE and X-ray photoelectron diffraction [61–64,69]. Both in terms of fundamental science, as well as for applications, one unanswered question is still whether cooperativity [72] effects play a role in the switching of these molecules within close-packed layers. To the best of our knowledge, cooperative switching of azobenzene switches has so far been observed only indirectly, i.e. via collective switching in certain areas [45], rather than following individual switching events over time. Addressing this question using spectroscopic techniques is difficult as they typically average over large numbers of molecules, and can therefore not resolve the behaviour of

\* Corresponding author at: Graz University of Technology, Experimental Physics, Coherent Sensing Group, Petersgasse 16, 8010 Graz, Austria.

\*\* Corresponding author at: University of Graz, Physical Chemistry Division, Heinrichstrasse 28, 8010 Graz, Austria.

E-mail addresses: [divora@tugraz.at](mailto:divora@tugraz.at) (R. di Vora), [matthew.timm@uni-graz.at](mailto:matthew.timm@uni-graz.at) (M.J. Timm), [leonhard.grill@uni-graz.at](mailto:leonhard.grill@uni-graz.at) (L. Grill), [schultze-bernhardt@tugraz.at](mailto:schultze-bernhardt@tugraz.at) (B. Bernhardt).

<https://doi.org/10.1016/j.susc.2026.122971>

Received 19 December 2025; Received in revised form 20 February 2026; Accepted 5 March 2026

Available online 6 March 2026

0039-6028/© 2026 The Authors. Published by Elsevier B.V. This is an open access article under the CC BY license (<http://creativecommons.org/licenses/by/4.0/>).

individual molecules. With STM, on the other hand, it is possible to image single molecules. However, statistical analysis requires STM imaging of large numbers of molecules, each characterized with sub-molecular resolution, which are very time-consuming to analyze – a challenge that can be tackled with a computer vision algorithm.

Here, we study the *trans-cis* switching events of individual azobenzene derivatives and investigate whether the presence of a switched molecule alters the switching likelihood of other azobenzene molecules in its vicinity, and whether cooperative phenomena are present. We demonstrate that STM imaging, when combined with a self-designed computer-vision algorithm, allows tracking of the isomeric configurations of thousands of mTBA molecules adsorbed in closely-packed islands on a Au(111) surface after repeated illuminations by pulsed laser radiation. The laser has a central wavelength of  $\lambda_c = (518 \pm 3)$  nm, corresponding to a frequency of approximately 0.6 MHz or 2.4 eV of photon energy at 80 MHz repetition rate. By tracking the switching behavior of a large amount of molecules we obtain evidence for the *trans-cis* isomerization of mTBA molecules being subject to surface effects.

## 2. Results and discussion

### 2.1. Appearance of *cis* and *trans* mTBA molecules in STM images

The mTBA molecules (see Fig. 1a for chemical structure) were deposited on the Au(111) surface as described in Methods. As can be seen in the STM shown in Fig. 1b, the surface exhibits prominent stripes parallel to the  $\langle 112 \rangle$  surface in an alternating herringbone-like pattern. This well-known herringbone structure arises from the presence of 23 surface Au atoms for every 22 bulk lattice constants along one of the  $\langle 110 \rangle$  directions [73–75]. Caused by this extra Au atom, a registry mismatch between the surface atoms and the underlying bulk lattice results in the surface Au atoms segregating into alternating face-centered cubic (fcc) and hexagonal close-packed (hcp) regions. Fcc and hcp regions are separated by ‘corrugation lines’ (striped features in Fig. 1b) with atoms that stick out of the surface by approximately 0.2 Å as compared to the fcc and hcp regions [73–75]. In Fig. 1b, the fcc regions, hcp regions and the corrugation lines between them are marked by yellow, blue, and magenta arrows, respectively.

On this surface with a surface coverage of 0.64 ML, *trans*-mTBA molecules, which lack an electric dipole moment or radicals, interact weakly via van der Waals interaction and self-assemble into large islands, some of which can contain many thousands of molecules. As an

example, the large island on the right of the STM image shown in Fig. 1c contains about 12,000 mTBA molecules. Within these islands, the molecules pack in parallel, staggered rows in which the long-axis of the molecule (indicated by a double-headed arrow in Fig. 1a lies at an angle of  $(4 \pm 3)^\circ$  to the  $[1\bar{1}0]$  surface direction [56,59]. The inset in Fig. 1c shows an individual *trans*-mTBA molecule highlighted by an orange box, surrounded by its local neighborhood of other *trans*-mTBA. The six nearest neighbor molecules are indicated by white rectangles.

Illumination of *trans*-mTBA adsorbed on Au(111), using wavelengths from 260 nm to 560 nm, has been shown to lead to molecular isomerization from the *trans* to the *cis* form [56,76]. Fig. 1d shows an STM image of the same area as Fig. 1c following illumination of the surface by a  $(518 \pm 3)$  nm (2.4 eV) pulsed laser (pulse length: 250 fs, repetition rate: 80 MHz), where the area was exposed to a total illumination time of 16 h. Following this illumination, >2500 mTBA molecules within the island have isomerized into the *cis* form. The inset in Fig. 1d shows the same mTBA molecule as Fig. 1c, though now in the *cis* configuration.

The adsorption configurations of the *trans* and *cis* mTBA molecules on Au(111) are well understood [36,54,56,57,60]: for the *cis*-configuration, one of the molecule’s four *tert*-butyl ‘legs’ sticks up and points away from the surface, while in the flatter *trans* configuration, all four *tert*-butyl ‘legs’ lie parallel to the surface [36,54,57,60,70]. This results in the two species having starkly different appearances in STM images. The *trans* species (Fig. 1c, inset) appears as a rectangular feature with two prominent lobes (apparent height 2.1 Å) on either side of a central linear depression which runs perpendicular to the molecule’s long axis. The prominent lobes correspond to the *tert*-butyl groups at either end of the molecule, while the dark line corresponds to the location of the  $N = N$  (Nitrogen double) bond [54,57,60]. The *cis* mTBA (Fig. 1d, inset) on the other hand has a central, prominent protrusion that appears approximately 1.5 Å higher as compared to the *trans* species, due to the upright *tert*-butyl ‘leg’.

The strong difference in appearance of *cis* and *trans* mTBA species in the STM images can readily be exploited by computer vision methods, which can analyze or retrieve data from recorded images [77], to automate identification of the location and isomeric state of each molecule. This enables direct tracking of the isomeric form of tens of thousands of individual molecules in collected STM images taken of the same areas over extended surface illumination periods.

### 2.2. Applying the computer vision algorithm to the data

The computer vision algorithm is described in the flowchart of Fig. 2

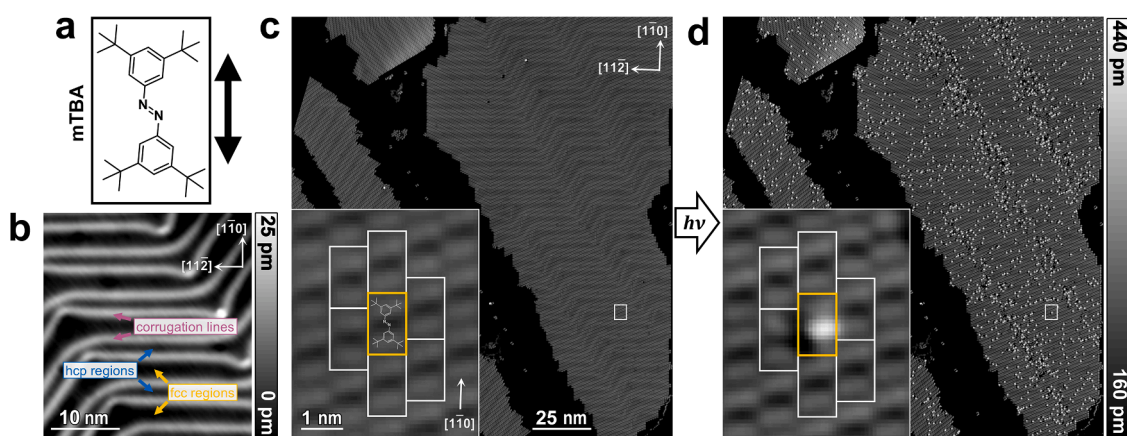


**Fig. 1.** Illumination by laser radiation induces *trans-cis* isomerization of mTBA on Au(111). a, Chemical structure of *trans*-mTBA with long-axis direction indicated by double-headed arrow. b, STM image of clean Au(111) surface with ‘herringbone’ reconstruction – important surface features are indicated with colored arrows. c-d, STM images of the same self-assembled islands of mTBA molecules (light grey) on the Au(111) surface. c, before and d after 16 h of illumination by a linearly polarized, pulsed laser beam ( $\lambda = 518$  nm). Insets in c-d show individual *trans*-mTBA and in d *cis* mTBA molecules (orange boxes) surrounded by their direct neighbors. Insets in c-d are zoomed-in views of the small white rectangles in the main images. In c-d the z-scale is the same for all images. Imaging conditions: b, 1.0 V, 100 pA, <6.0 K; c-d 0.4 V, 50 pA, < 7.0 K.

(each individual working step is described in detail in the Supplementary Material). Small, template images are used to identify molecules on larger STM images. Template images are small reference patches (STM image data of individual *cis* and *trans* molecules, see Figure S1 and S2) used to locate similar patterns on the larger images. From previous works, the appearance of *trans* and *cis* molecules is exactly known [54, 60]. The templates are subsequently used to carry out correlation calculations based on contrast differences [78]. The rectangular appearance with two prominent lobes appearing of either side of a central, linear depression of the *trans* isomer is more specific compared to the central, prominent protrusion of the *cis* isomer. We note that cursive molecules at the left-hand or right-hand edges of the mTBA islands (depending on the tip-approach direction) can artificially appear more prominent due to the responsiveness of the feed-back loop. Additionally, as reported in [57], there are four distinguishable ways the prominent lobe of a *cis* species can appear in an STM image. In contrast to the *cis* isomer, the appearance of the *trans* isomer does not resemble any other surface features, defects or contaminants. Thus, 5 template images were used for the *trans* isomer, and 10 template images were used for the *cis* isomer. The template images have manually been selected from the STM images to cover a range of variation in their appearance. The number of template images has been optimized, considering on the one hand a reliable set of templates and on the other hand the computational effort. An increase in the number of reference images would disproportionately increase the computational effort compared to the benefit received.

To reduce the complexity of the data for the computer vision algorithm, we perform alignment of the STM images before and after each illumination. This can be challenging, due to the large image sizes and slow acquisition times (> 25 min per image for sufficient image quality). Thermal drift, which is enhanced by the increased sample temperature during illumination (see Methods), and piezo creep can cause linear and non-linear skews which necessitate image-specific corrections. The first step of is to apply a plane subtraction and z-level alignment on each acquired STM image using the Gwyddion software [79]. Next, all images obtained for the same area were corrected by application of linear affine transformations (e.g. by translation, scaling, rotation and/or shearing) in data processing (available upon request).

The non-linear skew from piezo creep is strongest near the beginning of each acquired STM image (in this case, the top of the image), and this cannot be compensated by linear transformations. Thus, these parts of the images were masked out and not considered during analysis. Following these corrections, the features in each image were correctly aligned to within a few pixels (corresponding to about 2 Å). To improve the identification of individual molecules the contrast of the images is enhanced and masks to isolate the molecular islands are applied (compare Fig. 2a with Fig. 2b; see SI Figure S4a and S4b for further

examples). At this point the raw STM data (Fig. 2a; Figure S4a) is converted into a form that can be easily interpreted by the computer vision algorithm (Fig. 2b; Figure S4b).

The computer vision algorithm is applied to the corrected images to detect and label the location of each *trans* molecule, identifying the grid of *trans* mTBA molecules within the molecular islands. This can be seen in Fig. 2c, where each detected molecule is marked by a green rectangle. Importantly, this step of identifying the ‘*trans* grid’ is only performed for the first STM image taken of a given area (acquired prior to any surface illumination). Following each illumination (marked by ‘*hν*’ in Fig. 2), a computer vision algorithm specifically designed to detect individual *cis* species (Fig. 2d, blue rectangles) is utilized. The detected *cis* molecules and the *trans* grid are then combined to form a single ‘isomeric state’ grid (Fig. 2e), whereupon the isomeric state of each individual molecule is identified. It is worth reiterating that this approach enables us to track the isomeric state of every single molecule within a molecular island – some of which are composed of >10,000 individual mTBA molecules.

Finally, through comparing the isomeric state grids obtained before and after each illumination, the complete information about isomerization is available at the single-molecule level: which *trans* mTBA have newly become *cis* (Fig. 2f, magenta rectangles), which *cis* mTBA have returned to the *trans* state (Fig. 2f, yellow rectangle), and which *cis* and *trans* mTBA remain unchanged (Fig. 2f, blue and green rectangles, respectively). Thus, the isomerization of many molecules is simultaneously and accurately tracked over multiple illumination periods.

It is important to note that we initiate our experimental sequence with short illumination periods (2.5 min), corresponding to low isomerization rates. We can thus exclude multiple switching events (a *trans* → *cis* → *trans* isomerization sequence of the same molecule could for instance be interpreted wrongly as a non-switching molecule).

While the computer vision algorithm provides the individual coordinates of each molecule, it does not define their spatial relation to one another – this must be assigned through spatial transformations. Since the molecules follow a grid-like arrangement, such spatial transformations can be applied with great confidence. Using a near maximum suppression (NMS) algorithm, the rectangular area corresponding to a given molecule is shifted, for example upwards, by one unit the size of the rectangular area and its overlap with the rectangular areas of other detected molecules is calculated. The rectangular area calculated to have the highest overlap is then identified as the neighboring molecule. This allows the isomeric state (*cis* or *trans*) of each neighboring mTBA species to also be identified, and further it can be determined whether a particular mTBA is at the edge of, or within the molecular island.

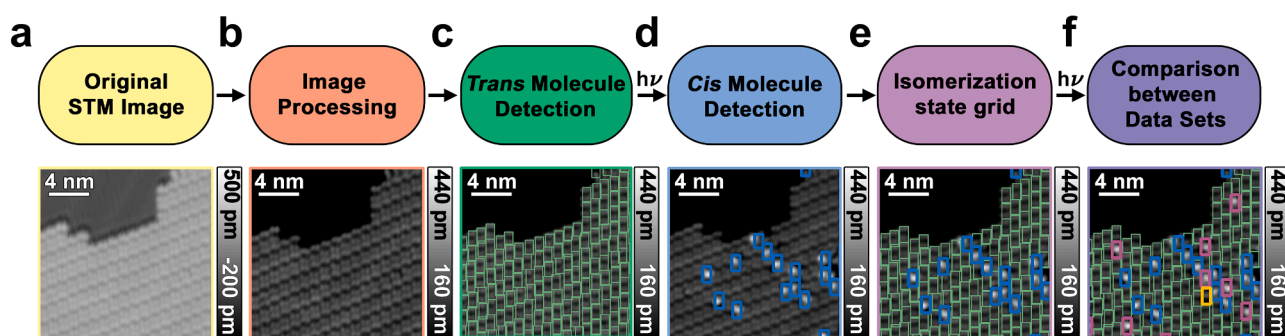


**Fig. 2.** Working steps of the computer vision algorithm. Shown are zoomed-in images of a larger molecular island (see SI Figure S4). (a) Original STM image. (b) STM image following processing to correct for skew, enhancing the contrast of the mTBA species, and placing a mask over everything but the object of interest (a single mTBA island). (c) Detection of *trans* molecules (green rectangles) by the computer vision algorithm. (d) Detection of *cis* molecules (blue rectangles) after illumination, indicated by *hν*. (e) Merger of cursive grid (from c) and *cis* grid (from d) to obtain isomeric state grid. (f) Comparison of isomeric state grids before and after a further illumination to identify newly occurring *cis* molecules (magenta rectangles), molecules transforming from *cis* back to *trans* (yellow rectangle), as well as unchanged *trans* and *cis* species (green and blue rectangles, respectively). Imaging conditions: 0.4 V, 50 pA, <7.0 K.

### 2.3. Nearest neighbors

It has been shown by Levy et al. [56] that the switching probability for mTBA can be influenced by molecular packing and the local electronic structure, as was particularly evident for islands comprised of different packing patterns. Particularly, for mTBA packed similarly to our samples, the authors state that the switching probability was completely random [56], however, our results show that this is not the case.

First, we study the location dependence of the switching probabilities of two directly neighboring mTBA molecules, one of them in the *cis* and the other in the *trans* configuration. In other words, we address whether the relative arrangement of the molecules to each other matter, i.e. on which side of the chemical structure the two molecules are located with respect to each other. If this was the case, then some of the neighbors in the close-packed arrangement in the islands would be preferred over others in their switching ability.

Each mTBA molecule has six direct neighboring molecules. Note, that owing to the three-fold rotational symmetry of the Au(111) surface (the corrugation lines of the herringbone reconstruction run along either of three (112) surface directions) and the mirror symmetry of how adjacent rows stagger (adjacent rows are displaced either ‘upwards’ or ‘downwards’), the data shown in this work has been folded to match the stacking shown in Fig. 1c. As illustrated in Fig. 3a, the six direct neighboring molecules form a ‘1<sup>st</sup> nearest-neighbor shell’ (colored in blue) and the next closest set of surrounding molecules form a ‘2<sup>nd</sup> nearest-neighbor shell’ (colored in magenta). For our location-dependent study, we name these neighbors N (north), NW (north-west), W (west), S (south), SE (south-east) and E (east) (Fig. 3a).

To identify how a given *cis* mTBA may affect the switching probability of its neighbor at each location, we impose three conditions on our analysis:

1. All mTBA species within the 1<sup>st</sup> and 2<sup>nd</sup> nearest-neighbor ‘shells’ surrounding a given *cis* mTBA molecule should be in the *trans* configuration at the start (i.e. prior to illumination).
2. Following an illumination, no molecules in the 2<sup>nd</sup> shell (magenta) should be in the *cis* configuration – that means the 2<sup>nd</sup> shell is still completely occupied by *trans* molecules. This condition is necessary, because if the 2<sup>nd</sup> shell was partially switched (i.e. a *cis* isomer appears), the new *cis* molecule could have more than one directly

neighboring *cis* species. In this case, we cannot know which *cis* species appeared first to influence the other.

3. Only one additional *cis* species has appeared within the 1<sup>st</sup> shell (as in Fig. 3b); cases in which multiple new *cis* molecules appear within the 1<sup>st</sup> shell are disregarded.

Multiple switches during one illumination period can occur (as the STM images can only capture the isomeric state at the very beginning and at the very end). However, due to the low isomerization rate for each illumination period, the occurrence of those multiple back and forth switches is small enough to be neglected (see above).

For comparability with prior work [54–60], we have focused on the switching probabilities for mTBA exhibiting the same packing patterns previously reported. It should be emphasized that at low surface coverage, such islands typically terminate where the corrugation lines change direction by 120°. However, at the high surface coverage investigated in this work (0.64 ML) we observe that these domains can also extend into regions where the corrugation lines change direction (this can be seen for the large island in Fig. 1c). Importantly, the switching in these extended domains was not considered in our analysis and molecules in these regions do not contribute to the data described below.

Fig. 3c displays the statistics that arise from this analysis, carried out on STM images acquired for four different areas of the surface, over up to 10 illumination periods. To compute this result, the switching behavior of thousands of individual molecules were surveyed over dozens of separate illuminations; though, given the imposed conditions described above, the total number of cases is low ( $N = 38$ ). A single case is defined as *cis* molecule, which has no other adjacent *cis* species (that is, within the 1<sup>st</sup> or 2<sup>nd</sup> ‘shells’), following illumination having a single new *cis* species appear within its 1<sup>st</sup> ‘shell’ and no new *cis* species appearing within the 2<sup>nd</sup> shell. In these cases, the location of an existing *cis* molecule defines where a second *cis* mTBA is likely to appear. We find that an additional *cis* molecule is most likely to be found at the NW and SE positions (Fig. 3c), with equal likelihood for both locations (13 instances NW, 14 SE). On the other hand, an additional *cis* was least likely to be found at the N and S positions, showing drastically smaller numbers (2 instances N, and 1 instance S). The E and W positions also showed a low likelihood to find an additional *cis* species (6 instances E, and 2 instances W – a difference which is close to the counting uncertainty, calculated as  $\sqrt{N}$  of the absolute count at each location). Most cases presented in Fig. 3c have the first *cis* molecule located at a fcc region. This is because more surface area is attributed to the fcc region,

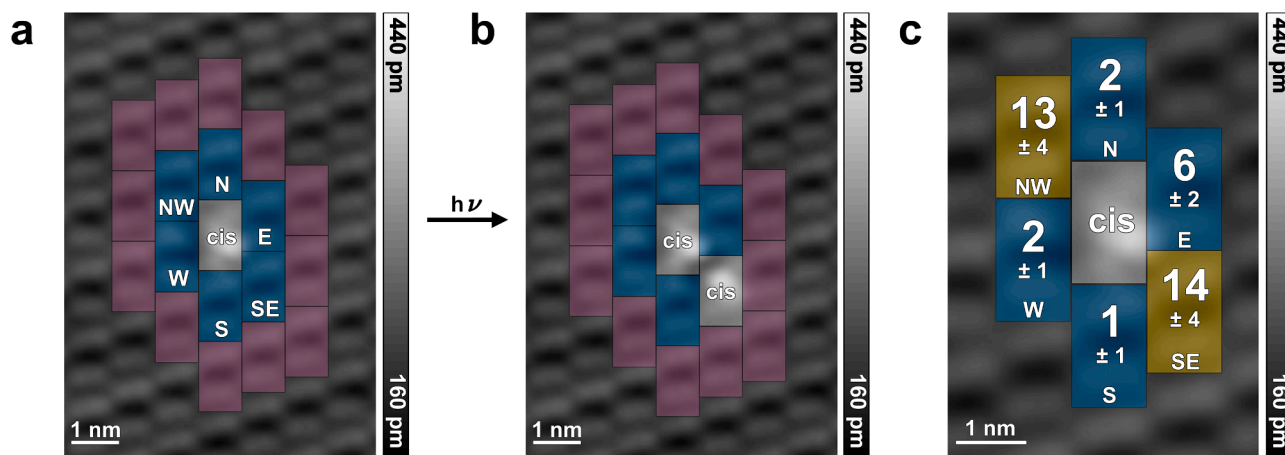


**Fig. 3.** Cumulative results of nearest-neighbor isomerization plotted over STM images. Results are obtained from analysis of 4 separate surface areas (with thousands of mTBA imaged per area), following multiple illuminations per area, and filtered according to conditions described in the text. The handedness of the mTBA as well as the appearance of the second *cis* molecules are not considered as part of this analysis. (a) An isolated *cis* mTBA surrounded by two ‘shells’ of *trans* mTBA species (blue: 1<sup>st</sup> shell; magenta: 2<sup>nd</sup> shell). (b) A single new *cis* mTBA occurring within the 1<sup>st</sup> shell. (c) Summation of positions within the first shell at which a newly occurring *cis* mTBA appears, with each neighboring position designated by a cardinal direction. The STM is the same as shown in (a). Imaging conditions: 0.4 V, 50 pA, <6.0 K.

while the hcp regions are very narrow in comparison and the lower isomerization probability for mTBA on corrugation lines.

To understand this, we applied our computer vision method to investigate whether the *cis* isomerization probability depends on the surface beneath each mTBA molecule similar like what has been observed for methoxy-substituted azobenzene on Au(111) [47]. As described above and shown in detail in Fig. 4, the reconstructed Au(111) surface consists of various regions that differ in the precise arrangement of the gold atoms. The molecules can adsorb either on the hcp or fcc areas, or on the corrugation lines (cl) that separate them (see Fig. 4). Importantly, it is known that the different arrangements of surface atoms in the fcc or hcp areas can affect the energetics of adsorbed molecules [80] and so could also affect the switching probability. We find that in the steady state, the quantity of *cis* isomers in these regions strongly differ: the fraction on the corrugation lines (Fig. 4, magenta), ( $7.4 \pm 0.9$  %), is much less than that for hcp, at ( $19.6 \pm 1.2$  %), (Fig. 4, blue) and fcc, at ( $22.5 \pm 0.8$  %), (Fig. 4, yellow) areas. The statistics are summarized in Table 1, shown below Fig. 4. We found that for the 38 cases tabulated in Fig. 3c, a second *cis* mTBA was most often found on a fcc or hcp region (approximately 90 % of cases).

Further, it was found that if the first *cis* mTBA was adsorbed upon a fcc or hcp region but adjacent to a corrugation line, then the second *cis* was never found upon the adjacent corrugation line. In other words, when a corrugation line was situated at the ‘north’ end of the first *cis*, then the second *cis* species was never found at the N or NW positions, and when the corrugation line was situated at the ‘south’ end of a *cis* mTBA, the second *cis* species was never found at the S or SE positions. With these findings we conclude that the corrugation line affects the *trans-cis* switching probability – likely due to the different surface structure as compared to the hcp and fcc regions [81,82]. Such a difference in the atomic arrangement can of course modify the adsorption configuration and consequently adsorption energy, which is important for the potential energy pathways for isomerization. Since these (fcc, hcp and cl) areas of the Au(111) surface are rather narrow with respect to the molecular size, these effects are very prominent for 1<sup>st</sup> and 2<sup>nd</sup> nearest neighbor shells (Fig. 3c). In terms of size, the fcc area between two corrugation lines can be approximately 2 nm wide, as compared to approximately 1 nm for the hcp region. The extent of the corrugation lines differs and is between 1 and 2 nm wide.

**Table 1**

The *cis*/total ratios are obtained from STM images taken of the steady state. The mTBA molecules above corrugation lines ( $N_{cis} = (220 \pm 60)$  out of  $N_{tot} = (2980 \pm 450)$ ) isomerize only half as often as ones above fcc ( $N_{cis} = (590 \pm 30)$  out of  $N_{tot} = (2640 \pm 240)$ ) or hcp regions ( $N_{cis} = (260 \pm 30)$  out of  $N_{tot} = (1300 \pm 220)$ ). See SI for discussion on uncertainties.

Surface Area	<i>cis</i> / total
face-centered cubic (fcc)	( $22.5 \pm 0.8$ %)
hexagonal close-packed (hcp)	( $19.6 \pm 1.2$ %)
corrugation line (cl)	( $7.4 \pm 0.9$ %)

### 3. Conclusions

The photo-induced isomerization of mTBA molecules in large, close-packed islands (consisting of up to approximately 10,000 individual mTBA molecules) was studied. To track the isomerization processes of so many molecules, an automated computer vision method has been developed. It allows precise tracking of the isomeric state (*trans* or *cis*) of every single azobenzene mTBA molecule in each STM image, thus allowing unprecedented access to switching statistics of individual mTBA molecules. With this applied imaging analysis, a previously unknown role of the gold corrugation line in quenching the *trans-cis* isomerization of mTBA was uncovered. mTBA molecules, if adsorbed on corrugation lines, display a drastically lower *trans-cis* isomerization probability. This study exemplifies how the use of computer vision can lead to new insights even in well-characterized systems like mTBA on Au (111).

### 4. Methods

#### 4.1. Experimental setup (STM)

The STM experiments are performed under ultra-high vacuum (UHV) conditions ( $p \leq 5.0 \times 10^{-10}$  mbar) using a low-temperature scanning tunneling microscope (CreaTec). The Au(111) crystal surface is prepared by sputtering the surface with Ar<sup>+</sup> ions ( $E = 1.85$  keV,  $p = 1.0 \times 10^{-5}$  mbar) and subsequently annealing the surface above 700 K under UHV conditions ( $p \leq 3.0 \times 10^{-9}$  mbar). The sputter-anneal cycles are repeated until a clean surface is obtained. This is monitored by repeated, intermediate STM imaging. Imaging of the surface is performed in

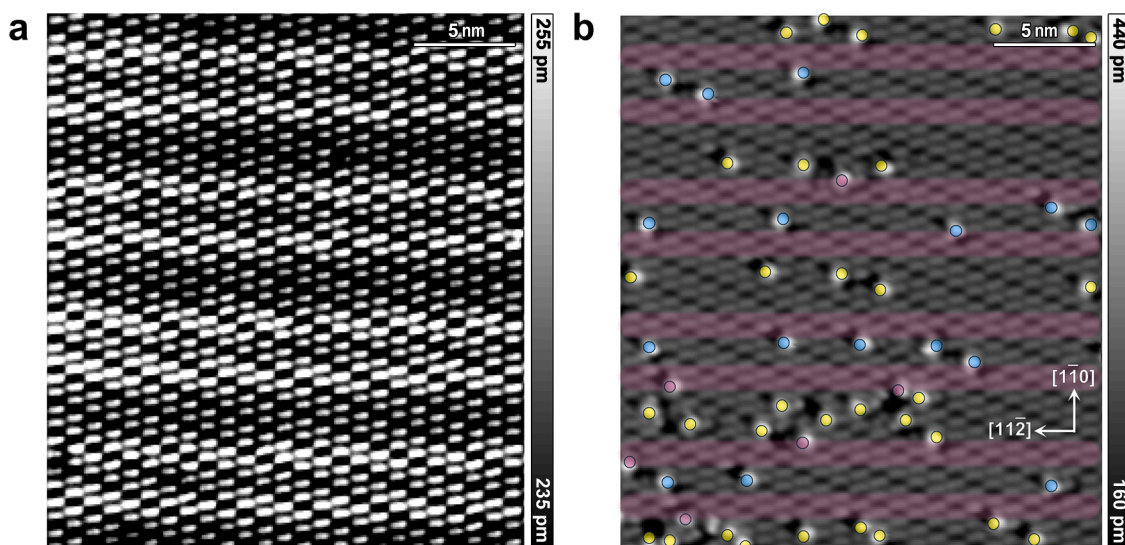


**Fig. 4.** Surface character affects mTBA isomerization probability. Beneath the molecular islands, the reconstructed Au(111) surface has three different areas: face-centered cubic (fcc, yellow) and hexagonal close-packed (hcp, blue) areas, and the corrugation lines (cl, magenta) that separate them. a shows the original STM image with high contrast to emphasize the corrugation lines. b has the surface areas color coded and *cis* molecules marked.

constant-current mode at temperatures  $< 6.0$  K using a platinum-iridium STM tip, which is conditioned through controlled crashing into clean patches of the Au surface. STM images were visualized using the Gwyddion Software [79].

The molecule, 3,3',5,5'-tetra-*tert*-butylazobenzene (mTBA; chemical structure given in Fig. 1a), is deposited onto the clean Au(111) surface, located at the STM stage and therefore kept at a temperature below 7.0 K, using a Si-wafer evaporator (current: 0.16 A, voltage: 6.0 V, deposition time: 140 s), resulting in a coverage of about 0.64 monolayers. To achieve the formation of large, well-ordered, self-assembled islands of almost exclusively ( $> 99.95\%$ ) *trans* mTBA molecules (see Fig. 1b), the Au(111) sample is warmed up to room temperature for a few minutes. Previous work has shown that heating to temperatures above 200 K results in almost complete conversion of *cis* mTBA molecules to the *trans* conformer [76].

#### 4.2. Experimental setup (Laser)

We employ a commercial femtosecond Yb: fiber laser from Menlo Systems, with a central wavelength of 1035 nm, full width half maximum of 6 nm, a repetition rate of 80 MHz and a pulse duration of 250 fs. The infrared output is frequency-doubled in a LBO crystal to  $(518 \pm 3)$  nm (2.4 eV), with a spectral bandwidth (FWHM) of  $T = 3$  nm. An optical bandpass filter and dichroic mirrors remove the infrared component before the green beam is directed into the STM system. A 500 mm focal length lens focuses the beam onto the sample to enhance the intensity at the sample. The angle of incidence onto the sample is approximately 60 degrees to the surface normal. The average power used during the experiments (measured in front of the vacuum chamber) is  $P = (7.7 \pm 0.1)$  mW. About 92 % of the beam power passes through the vacuum window into the chamber and onto the sample.

#### 4.3. Illumination procedure

Prior to the first illumination, a high-resolution STM-image (image resolution: 110 pixels/nm<sup>2</sup>) is acquired for a large area of the surface (larger than 100 nm  $\times$  100 nm). The STM tip is then retracted by macroscopic distances (by approx. 0.5 cm - 1 cm) and the laser is focused onto the Au(111) surface, on the area beneath the STM tip. Via camera, a spot diameter of  $(1.1 \pm 0.2)$  mm is measured on the sample. The spot was positioned to have its center at the position of the STM tip when the tip is at the surface. Reproducibility of spot positioning was monitored via camera and via the projection of the reflected beam onto the lab wall. Thus, movement of the beam and changes in the alignment could be documented and compensated. During illumination, the sample temperature rises from its base temperature of  $< 6.0$  K up to a maximum of 7.8 K for long illumination times ( $> 12$  h). Following illumination, the tip is re-approached to the surface and the same area is scanned. The above procedure is repeated for up to ten illuminations of the same area.

#### 4.4. Automatically detecting molecules and their isomeric states

The computer vision algorithm is based upon correlation calculations (TM\_CCOCOFF\_NORMED) using the opensource Python library cv2 [78]. A Non-Maximum-Suppression (NMS) algorithm is used to compensate for doublecounting of the same molecules. An additional brightness filter limits the number of false-positive results. This computer vision implementation was chosen because it can run on a local machine – even with the large data sets used in this work. A detailed explanation of the individual steps of the computer vision algorithm is provided in the supplementary material. A commented and generalized version of the used Python code is available upon request. The training data for the computer vision algorithm is available alongside an explanation in Figure S1 and S2 in the supplementary material.

## Funding

This project has received funding from the European Research Council (ERC) under the European Union's Horizon 2020 research and innovation programme (grant numbers 947288 and 101097326) as well as from the FWF (Austrian Science Fund, project numbers I 4897-N, I 5145-N and ESP 473-N). Financial support from the German Research Foundation (DFG via CRC 1636 "Elementary Processes of Light-Driven Reactions at Nanoscale Metals") is gratefully acknowledged. S.H. is indebted to the Einstein Foundation Berlin as well as Humboldt University for generous support.

## CRediT authorship contribution statement

**Robert di Vora:** Writing – review & editing, Writing – original draft, Visualization, Validation, Software, Methodology, Investigation, Formal analysis, Data curation, Conceptualization. **Matthew James Timm:** Writing – review & editing, Writing – original draft, Visualization, Validation, Methodology, Investigation, Funding acquisition, Formal analysis, Data curation, Conceptualization. **Alexander Eber:** Writing – review & editing, Validation, Methodology, Conceptualization. **Emily Hruska:** Writing – review & editing, Validation, Supervision. **Stefan Hecht:** Writing – review & editing, Validation, Resources, Funding acquisition. **Leonhard Grill:** Writing – review & editing, Validation, Supervision, Project administration, Methodology, Investigation, Funding acquisition, Conceptualization. **Birgitta Bernhardt:** Writing – review & editing, Validation, Supervision, Resources, Project administration, Investigation, Funding acquisition, Conceptualization.

## Declaration of competing interest

The authors declare that they have no known competing financial interests or personal relationships that could have appeared to influence the work reported in this paper.

## Acknowledgments

We gratefully acknowledge Christophe Nacci for help during the STM experiments. Jutta Schwarz is acknowledged for help with the synthesis of meta-TBA.

## Supplementary materials

Supplementary material associated with this article can be found, in the online version, at doi:10.1016/j.susc.2026.122971.

## Data availability

Data will be made available on request.

## References

- [1] A.K. Schnack-Petersen, M. Pápai, K.B. Møller, Azobenzene photoisomerization dynamics: revealing the key degrees of freedom and the long timescale of the *trans*-to-*cis* process, *J. Photochem. Photobiol. Chem.* 428 (2022) 113869, <https://doi.org/10.1016/j.jphotochem.2022.113869>.
- [2] B. Zhang, Y. Feng, W. Feng, Azobenzene-based solar thermal fuels: a review, *Nanomicro Lett.* 14 (2022) 138, <https://doi.org/10.1007/s40820-022-00876-8>.
- [3] I.C.D. Merritt, D. Jacquemin, M. Vacher, *cis*  $\rightarrow$  *trans* photoisomerisation of azobenzene: a fresh theoretical look, *Phys. Chem. Chem. Phys.* 23 (2021) 19155–19165, <https://doi.org/10.1039/D1CP01873F>.
- [4] J.D. Steen, D.R. Duijnste, W.R. Browne, Molecular switching on surfaces, *Surf. Sci. Rep.* 78 (2023) 100596, <https://doi.org/10.1016/j.surfrep.2023.100596>.
- [5] D. Pirone, N.A.G. Bandeira, B. Tylkowski, E. Boswell, R. Labeque, R. Garcia Valls, M. Giamberini, Contrasting photo-switching rates in azobenzene derivatives: how the nature of the substituent plays a role, *Polym. (Basel)* 12 (2020) 1019, <https://doi.org/10.3390/polym12051019>.
- [6] J. Sun, F. Wang, H. Zhang, K. Liu, Azobenzene-based photomechanical biomaterials, *Adv. Nanobiomed Res.* 1 (2021) 2100020, <https://doi.org/10.1002/anbr.202100020>.

- [7] Y. Feng, K. Zhang, X. Gao, W. Yang, J. Wan, H. Fu, H. Guo, Z. Li, Recent advances in photopharmacology: harnessing visible light-activated azobenzene photoswitches, *Responsive Mater.* 3 (2025) e20250003, <https://doi.org/10.1002/rpm.20250003>.
- [8] J. Ding, Z. Huang, D. Zhang, Y. Qu, S. Zhang, C. Zhang, B. Fang, L. Li, W. Huang, Rational structural design of aromatic azo photoactive small molecules for biomedical applications, *Chem. Soc. Rev.* 54 (2025) 10363–10396, <https://doi.org/10.1039/D5CS00334B>.
- [9] M. Di Martino, L. Sessa, R. Diana, S. Pianto, S. Concilio, Recent progress in photoresponsive biomaterials, *Molecules.* 28 (2023) 3712, <https://doi.org/10.3390/molecules28093712>.
- [10] P.P. Birnbaum, D.W.G. Style, The photo-isomerization of some azobenzene derivatives, *Trans. Faraday Soc.* 50 (1954) 1192, <https://doi.org/10.1039/TF9545001192>.
- [11] A.K. Bartholomew, I.B. Stone, M.L. Steigerwald, T.H. Lambert, X. Roy, Highly twisted Azobenzene Ligand causes crystals to continuously roll in sunlight, *J. Am. Chem. Soc.* 144 (2022) 16773–16777, <https://doi.org/10.1021/jacs.2c08815>.
- [12] J. Mahmoud Halabi, E. Ahmed, S. Sofela, P. Naumov, Performance of molecular crystals in conversion of light to mechanical work, *Proc. Natl. Acad. Sci.* 118 (2021) e2020604118, <https://doi.org/10.1073/pnas.2020604118>.
- [13] C. He, Y. Xiao, S. Wang, H. Lu, X. Li, L. Xu, C. Wang, Y. Tu, Main-chain azobenzene poly(ether ester) multiblock copolymers for strong and tough light-driven actuators, *ACS Appl. Mater. Interfaces* 16 (2024) 56469–56480, <https://doi.org/10.1021/acsmi.4c13375>.
- [14] K. Saito, K. Ichihyanagi, S. Nozawa, R. Haruki, D. Fan, T. Kanazawa, Y. Norikane, Transportation of nano/microparticles via photoinduced crawling of azobenzene crystals, *Adv. Mater. Interfaces* 10 (2023) 2202525, <https://doi.org/10.1002/admi.202202525>.
- [15] P. Dietrich, F. Michalik, R. Schmidt, C. Gahl, G. Mao, M. Breusing, M.B. Raschke, B. Prieswisch, T. Elsässer, R. Mendelsohn, M. Weinelt, K. Rück-Braun, An anchoring strategy for photoswitchable biosensor technology: azobenzene-modified SAMs on Si(111), *Applied Physics A* 93 (2008) 285–292, <https://doi.org/10.1007/s00339-008-4828-0>.
- [16] M. Sahanawaz, M.L. Maity, S. Koppayithodi, S. Bandyopadhyay, A smart photoswitchable sensor for differential detection of multiple nucleotides in two photoswitchable states using machine learning techniques, *Anal. Sens.* 6 (2026), <https://doi.org/10.1002/anse.202500082>.
- [17] M. Min, S. Seo, S.M. Lee, H. Lee, Voltage-controlled nonvolatile molecular memory of an azobenzene monolayer through solution-processed reduced graphene oxide contacts, *Adv. Mater.* 25 (2013) 7045–7050, <https://doi.org/10.1002/adma.201303335>.
- [18] A. Boschi, S. Cinili, E. Bystrenova, G. Ruani, J. Groppi, A. Credi, M. Baroncini, A. Candini, D. Gentili, M. Cavallini, Multimodal sensing in rewritable, data matrix azobenzene-based devices, *J. Mater. Chem. C Mater.* 10 (2022) 10132–10138, <https://doi.org/10.1039/D2TC01565J>.
- [19] T. Koehler, I. Strauss, A. Mundstock, J. Caro, F. Marlow, Reversible photoalignment of Azobenzene in the SURMOF HKUST-1, *J. Phys. Chem. Lett.* 12 (2021) 8903–8908, <https://doi.org/10.1021/acs.jpclett.1c02489>.
- [20] S. Sahu, S.K. Behera, Tuning molecular assembly to enhance azobenzene-based solar thermal fuel efficiency, *J. Mater. Chem. C Mater.* 13 (2025) 3167–3192, <https://doi.org/10.1039/D4TC02993C>.
- [21] C.-W. Chang, Y.-C. Lu, T.-T. Wang, E.W.-G. Diao, Photoisomerization dynamics of azobenzene in solution with S1 excitation: a femtosecond fluorescence anisotropy study, *J. Am. Chem. Soc.* 126 (2004) 10109–10118, <https://doi.org/10.1021/ja049215p>.
- [22] W.S. Struve, Emission from the  $1(n, \pi^*)$  state of azobenzene: spectrum and ultrashort decay time, *Chem. Phys. Lett.* 46 (1977) 15–19, [https://doi.org/10.1016/0009-2614\(77\)85154-3](https://doi.org/10.1016/0009-2614(77)85154-3).
- [23] C.G. Morgante, W.S. Struve, S2 → S0 fluorescence in trans-azobenzene, *Chem. Phys. Lett.* 68 (1979) 267–271, [https://doi.org/10.1016/0009-2614\(79\)87198-5](https://doi.org/10.1016/0009-2614(79)87198-5).
- [24] H. Rau, Further evidence for rotation in the  $\pi, \pi^*$  and inversion in the  $n, \pi^*$  photoisomerization of azobenzenes, *J. Photochem.* 26 (1984) 221–225, [https://doi.org/10.1016/0047-2670\(84\)80041-6](https://doi.org/10.1016/0047-2670(84)80041-6).
- [25] A.A. Beharry, O. Sadovski, G.A. Woolley, Azobenzene photoswitching without ultraviolet light, *J. Am. Chem. Soc.* 133 (2011) 19684–19687, <https://doi.org/10.1021/ja209239m>.
- [26] J. Griffiths, II. Photochemistry of azobenzene and its derivatives, *Chem. Soc. Rev.* 1 (1972) 481–493, <https://doi.org/10.1039/CS9720100481>.
- [27] N. Siampiringue, G. Guyot, S. Monti, P. Bortolus, The cis → trans photoisomerization of azobenzene: an experimental re-examination, *J. Photochem.* 37 (1987) 185–188, [https://doi.org/10.1016/0047-2670\(87\)85039-6](https://doi.org/10.1016/0047-2670(87)85039-6).
- [28] J. Wachtveitl, S. Spörlein, H. Satzger, B. Fonrobert, C. Renner, R. Behrendt, D. Oesterhelt, L. Moroder, W. Zinth, Ultrafast conformational dynamics in cyclic azobenzene peptides of increased flexibility, *Biophys. J.* 86 (2004) 2350–2362, [https://doi.org/10.1016/S0006-3495\(04\)74292-7](https://doi.org/10.1016/S0006-3495(04)74292-7).
- [29] A. Safiei, J. Henzl, K. Morgenstern, Isomerization of an azobenzene derivative on a thin insulating layer by inelastically tunneling electrons, *Phys. Rev. Lett.* 104 (2010) 216102, <https://doi.org/10.1103/PhysRevLett.104.216102>.
- [30] S. Jaekel, A. Richter, R. Lindner, R. Bechstein, C. Nacci, S. Hecht, A. Kühnle, L. Grill, Reversible and efficient light-induced molecular switching on an insulator surface, *ACS. Nano.* 12 (2018) 1821–1828, <https://doi.org/10.1021/acsnano.7b08624>.
- [31] N. Henningsen, R. Rurali, K.J. Franke, I. Fernández-Torrente, J.I. Pascual, Trans to cis isomerization of an azobenzene derivative on a Cu(100) surface, *Appl. Phys. A* 93 (2008) 241–246, <https://doi.org/10.1007/s00339-008-4840-4>.
- [32] E. McNellis, J. Meyer, A.D. Baghi, K. Reuter, Stabilizing a molecular switch at solid surfaces: a density functional theory study of azobenzene on Cu(111), Ag(111), and Au(111), *Phys. Rev. B.* 80 (2009) 35414, <https://doi.org/10.1103/PhysRevB.80.035414>.
- [33] E.R. McNellis, J. Meyer, K. Reuter, Azobenzene at coinage metal surfaces: role of dispersive van der Waals interactions, *Phys. Rev. B.* 80 (2009) 205414, <https://doi.org/10.1103/PhysRevB.80.205414>.
- [34] G. Mercurio, E.R. McNellis, I. Martin, S. Hagen, F. Leyssner, S. Soubatch, J. Meyer, M. Wolf, P. Tegeder, F.S. Tautz, K. Reuter, Structure and energetics of Azobenzene on Ag(111): benchmarking semiempirical dispersion correction approaches, *Phys. Rev. Lett.* 104 (2010) 36102, <https://doi.org/10.1103/PhysRevLett.104.036102>.
- [35] E.R. McNellis, G. Mercurio, S. Hagen, F. Leyssner, J. Meyer, S. Soubatch, M. Wolf, K. Reuter, P. Tegeder, F.S. Tautz, Bulky spacer groups – a valid strategy to control the coupling of functional molecules to surfaces? *Chem. Phys. Lett.* 499 (2010) 247–249, <https://doi.org/10.1016/j.cpllet.2010.09.051>.
- [36] E.R. McNellis, C. Bronner, J. Meyer, M. Weinelt, P. Tegeder, K. Reuter, Azobenzene versus 3,3',5,5'-tetra-tert-butyl-azobenzene (TBA) at Au(111): characterizing the role of spacer groups, *Phys. Chem. Chem. Phys.* 12 (2010) 6404–6412, <https://doi.org/10.1039/C001978J>.
- [37] C.J. Xia, H.C. Liu, C.F. Fang, The IV characteristics of the 3, 3', 5', 5'-tetra-tert-butyl-azobenzene optical molecular switch: a first-principles study, *Adv. Mat. Res.* 152 (2011) 839–842, <https://doi.org/10.4028/www.scientific.net/AMR.152-153.839>.
- [38] I.V. Pechenezhskiy, J. Cho, G.D. Nguyen, L. Berbil-Bautista, B.L. Giles, D. A. Poulsen, J.M.J. Fréchet, M.F. Crommie, Self-assembly and photomechanical switching of an azobenzene derivative on GaAs(110): scanning tunneling microscopy study, *J. Phys. Chem. C.* 116 (2012) 1052–1055, <https://doi.org/10.1021/jp209835n>.
- [39] H. Birla, S.H. Mir, K. Yadav, T. Halbritter, A. Heckel, J.K. Singh, T.G. Gopakumar, Unusual one dimensional cascade effect in the thermal and photo-induced switching of azobenzene derivatives on a graphite surface, *Chem. Sci.* 16 (2025) 6325–6335, <https://doi.org/10.1039/D4SC07570F>.
- [40] S. Jaekel, R. Stoll, F. Berger, S. Hecht, L. Grill, Azobenzene isomerization on a reactive copper surface by efficient decoupling with bulky side groups, *Surf. Sci.* 744 (2024) 122468, <https://doi.org/10.1016/j.susc.2024.122468>.
- [41] M. Ai, S. Groeper, W. Zhuang, X. Dou, X. Feng, K. Müllen, J.P. Rabe, Optical switching studies of an azobenzene rigidly linked to a hexa-peri-hexabenzocoronene derivative in solution and at a solid–liquid interface, *Appl. Phys. A.* 93 (2008) 277–283, <https://doi.org/10.1007/s00339-008-4871-x>.
- [42] A. Kirakosian, M.J. Comstock, J. Cho, M.F. Crommie, Molecular commensurability with a surface reconstruction: STM study of azobenzene on Au(111), *Phys. Rev. B.* 71 (2005) 113409, <https://doi.org/10.1103/PhysRevB.71.113409>.
- [43] M.J. Comstock, J. Cho, A. Kirakosian, M.F. Crommie, Manipulation of azobenzene molecules on Au(111) using scanning tunneling microscopy, *Phys. Rev. B.* 72 (2005) 153414, <https://doi.org/10.1103/PhysRevB.72.153414>.
- [44] J. Henzl, M. Mehlhorn, H. Gawronski, K.-H. Rieder, K. Morgenstern, Reversible cis–trans isomerization of a single azobenzene molecule, *Angew. Chem. Int. Ed.* 45 (2006) 603–606, <https://doi.org/10.1002/anie.200502229>.
- [45] G. Pace, V. Ferri, C. Grave, M. Elbing, C. von Hänisch, M. Zharnikov, M. Mayor, M. A. Rampi, P. Samorì, Cooperative light-induced molecular movements of highly ordered azobenzene self-assembled monolayers, *Proc. Natl. Acad. Sci.* 104 (2007) 9937–9942, <https://doi.org/10.1073/pnas.0703748104>.
- [46] N. Henningsen, K.J. Franke, G. Schulze, I. Fernández-Torrente, B. Prieswisch, K. Rück-Braun, J.I. Pascual, Active intramolecular conformational dynamics controlling the assembly of azobenzene derivatives at surfaces, *Chemphyschem.* 9 (2008) 71–73, <https://doi.org/10.1002/cphc.200700678>.
- [47] C. Dri, M.V. Peters, J. Schwarz, S. Hecht, L. Grill, Spatial periodicity in molecular switching, *Nat. Nanotechnol.* 3 (2008) 649–653, <https://doi.org/10.1038/nnano.2008.269>.
- [48] S. Selvanathan, M.V. Peters, J. Schwarz, S. Hecht, L. Grill, Formation and manipulation of discrete supramolecular azobenzene assemblies, *Appl. Phys. A* 93 (2008) 247–252, <https://doi.org/10.1007/s00339-008-4827-1>.
- [49] J. Cho, N. Levy, A. Kirakosian, M.J. Comstock, F. Lauterwasser, J.M.J. Fréchet, M. F. Crommie, Surface anchoring and dynamics of thiolated azobenzene molecules on Au(111), *J. Chem. Phys.* 131 (2009) 34707, <https://doi.org/10.1063/1.3168524>.
- [50] J. Henzl, K. Morgenstern, An electron induced two-dimensional switch made of azobenzene derivatives anchored in supramolecular assemblies, *Phys. Chem. Chem. Phys.* 12 (2010) 6035–6044, <https://doi.org/10.1039/B924488C>.
- [51] J. Mielke, S. Selvanathan, M. Peters, J. Schwarz, S. Hecht, L. Grill, Molecules with multiple switching units on a Au(111) surface: self-organization and single-molecule manipulation, *J. Phys.: Condens. Matter.* 24 (2012) 394013, <https://doi.org/10.1088/0953-8984/24/39/394013>.
- [52] C. Nacci, M. Baroncini, A. Credi, L. Grill, Reversible photoswitching and isomer-dependent diffusion of single azobenzene tetramers on a metal surface, *Angew. Chem. Int. Ed.* 57 (2018) 15034–15039, <https://doi.org/10.1002/anie.201806536>.
- [53] T.R. Rusch, A. Schlimm, N.R. Krekhihn, T. Tellkamp, S. Budzák, D. Jacquemin, F. Tuczek, R. Herges, O.M. Magnussen, Observation of collective photoswitching in free-standing TATA-based azobenzenes on Au(111), *Angew. Chem. Int. Ed.* 59 (2020) 17192–17196, <https://doi.org/10.1002/anie.202003797>.
- [54] M.J. Comstock, N. Levy, A. Kirakosian, J. Cho, F. Lauterwasser, J.H. Harvey, D. A. Strubbe, J.M.J. Fréchet, D. Trauner, S.G. Louie, M.F. Crommie, Reversible photomechanical switching of individual engineered molecules at a metallic surface, *Phys. Rev. Lett.* 99 (2007) 038301, <https://doi.org/10.1103/PhysRevLett.99.038301>.

- [55] M.J. Comstock, N. Levy, J. Cho, L. Berbil-Bautista, M.F. Crommie, D.A. Poulsen, J. M.J. Fréchet, Measuring reversible photomechanical switching rates for a molecule at a surface, *Appl. Phys. Lett.* 92 (2008) 123107, <https://doi.org/10.1063/1.2901877>.
- [56] N. Levy, M.J. Comstock, J. Cho, L. Berbil-Bautista, A. Kirakosian, F. Lauterwasser, D.A. Poulsen, J.M.J. Fréchet, M.F. Crommie, Self-patterned molecular photoswitching in nanoscale surface assemblies, *Nano Lett.* 9 (2009) 935–939, <https://doi.org/10.1021/nl802632g>.
- [57] M.J. Comstock, D.A. Strubbe, L. Berbil-Bautista, N. Levy, J. Cho, D. Poulsen, J.M. J. Fréchet, S.G. Louie, M.F. Crommie, Determination of photoswitching dynamics through chiral mapping of single molecules using a scanning tunneling microscope, *Phys. Rev. Lett.* 104 (2010) 178301, <https://doi.org/10.1103/PhysRevLett.104.178301>.
- [58] S. Godey, H. Therssen, D. Guérin, T. Mélin, S. Lenfant, Electroisomerization blinking of an azobenzene derivative molecule, *Nanotechnology*. 36 (2025) 105702, <https://doi.org/10.1088/1361-6528/ada2f3>.
- [59] M. Alemanni, M.V. Peters, S. Hecht, K.-H. Rieder, F. Moresco, L. Grill, Electric field-induced isomerization of azobenzene by STM, *J. Am. Chem. Soc.* 128 (2006) 14446–14447, <https://doi.org/10.1021/ja065449s>.
- [60] M. Alemanni, S. Selvanathan, F. Ample, M.V. Peters, K.-H. Rieder, F. Moresco, C. Joachim, S. Hecht, L. Grill, Adsorption and switching properties of azobenzene derivatives on different noble metal surfaces: Au(111), Cu(111), and Au(100), *J. Phys. Chem. C*. 112 (2008) 10509–10514, <https://doi.org/10.1021/jp711134p>.
- [61] S. Hagen, F. Leyssner, D. Nandi, M. Wolf, P. Tegeder, Reversible switching of tetra-tert-butyl-azobenzene on a Au(111) surface induced by light and thermal activation, *Chem. Phys. Lett.* 444 (2007) 85–90, <https://doi.org/10.1016/j.cplett.2007.07.005>.
- [62] L. Óvári, M. Wolf, P. Tegeder, Reversible changes in the vibrational structure of tetra-tert-butylazobenzene on a Au(111) surface induced by light and thermal activation, *J. Phys. Chem. C*. 111 (2007) 15370–15374, <https://doi.org/10.1021/jp075274o>.
- [63] S. Hagen, P. Kate, F. Leyssner, D. Nandi, M. Wolf, P. Tegeder, Excitation mechanism in the photoisomerization of a surface-bound azobenzene derivative: role of the metallic substrate, *J. Chem. Phys.* 129 (2008) 164102, <https://doi.org/10.1063/1.2997343>.
- [64] S. Hagen, P. Kate, M.V. Peters, S. Hecht, M. Wolf, P. Tegeder, Kinetic analysis of the photochemically and thermally induced isomerization of an azobenzene derivative on Au(111) probed by two-photon photoemission, *Appl. Phys. A*. 93 (2008) 253–260, <https://doi.org/10.1007/s00339-008-4831-5>.
- [65] M. Piantek, J. Miguel, M. Bernien, C. Navio, A. Krüger, B. Prieswisch, K. Rück-Braun, W. Kuch, Adsorption of carboxymethylester-azobenzene on copper and gold single crystal surfaces, *Appl. Phys. A*. 93 (2008) 261–266, <https://doi.org/10.1007/s00339-008-4825-3>.
- [66] R. Schmidt, E. McNellis, W. Freyer, D. Brete, T. Gießel, C. Gahl, K. Reuter, M. Weinelt, Azobenzene-functionalized alkanethiols in self-assembled monolayers on gold, *Appl. Phys. A*. 93 (2008) 267–275, <https://doi.org/10.1007/s00339-008-4829-z>.
- [67] C. Gahl, R. Schmidt, D. Brete, E.R. McNellis, W. Freyer, R. Carley, K. Reuter, M. Weinelt, Structure and excitonic coupling in self-assembled monolayers of azobenzene-functionalized alkanethiols, *J. Am. Chem. Soc.* 132 (2010) 1831–1838, <https://doi.org/10.1021/ja903636q>.
- [68] B.-Y. Choi, S.-J. Kahng, S. Kim, H. Kim, H.W. Kim, Y.J. Song, J. Ihm, Y. Kuk, Conformational molecular switch of the azobenzene molecule: a scanning tunneling microscopy study, *Phys. Rev. Lett.* 96 (2006) 156106, <https://doi.org/10.1103/PhysRevLett.96.156106>.
- [69] A. Schuler, M. Greif, A.P. Seitsonen, G. Mette, L. Castiglioni, J. Osterwalder, M. Hengsberger, Sensitivity of photoelectron diffraction to conformational changes of adsorbed molecules: tetra-tert-butyl-azobenzene/Au(111), *Struct. Dyn.* 4 (2017) 15101, <https://doi.org/10.1063/1.4975594>.
- [70] R. Schmidt, S. Hagen, D. Brete, R. Carley, C. Gahl, J. Dokić, P. Saalfrank, S. Hecht, P. Tegeder, M. Weinelt, On the electronic and geometrical structure of the trans- and cis-isomer of tetra-tert-butyl-azobenzene on Au(111), *Phys. Chem. Chem. Phys.* 12 (2010) 4488–4497, <https://doi.org/10.1039/B924409C>.
- [71] T. Sassmannshausen, N. Oberhof, M.A. Strauss, C. Slavov, H.A. Wegner, A. Dreuw, J. Wachtveitl, Dispersion-controlled excited-state dynamics in Azobenzene photoisomerization, *J. Am. Chem. Soc.* 148 (2026) 997–1003, <https://doi.org/10.1021/jacs.5c16915>.
- [72] C.A. Hunter, H.L. Anderson, What is cooperativity? *Angew. Chem. Int. Ed.* 48 (2009) 7488–7499, <https://doi.org/10.1002/anie.200902490>.
- [73] J.V. Barth, H. Brune, G. Ertl, R.J. Behm, Scanning tunneling microscopy observations on the reconstructed Au(111) surface: atomic structure, long-range superstructure, rotational domains, and surface defects, *Phys. Rev. B*. 42 (1990) 9307–9318, <https://doi.org/10.1103/PhysRevB.42.9307>.
- [74] Ch. Wöll, S. Chiang, R.J. Wilson, P.H. Lippel, Determination of atom positions at stacking-fault dislocations on Au(111) by scanning tunneling microscopy, *Phys. Rev. B*. 39 (1989) 7988–7991, <https://doi.org/10.1103/PhysRevB.39.7988>.
- [75] P. Li, F. Ding, Origin of the herringbone reconstruction of Au(111) surface at the atomic scale, *Sci. Adv.* 8 (2022) eabq2900, <https://doi.org/10.1126/sciadv.abq2900>.
- [76] S. Hagen, Isomerization behavior of photochromic molecules in direct contact with noble metal surfaces, 2009. <http://dx.doi.org/10.17169/refubium-18134>.
- [77] R. Klette, Concise computer vision - an introduction into theory and algorithms, 1st ed, Springer London, Springer-Verlag London Ltd., part of Springer Nature, 2014, p. 2014, <https://doi.org/10.1007/978-1-4471-6320-6>.
- [78] G. Bradski, The OpenCV Library, Dr. Dobb's J. Softw. Tools (2000), in: [https://docs.opencv.org/4.9.0/df/dfb/group\\_imgproc\\_object.html](https://docs.opencv.org/4.9.0/df/dfb/group_imgproc_object.html).
- [79] D. Nečas, P. Klapetek, Gwyddion: an open-source software for SPM data analysis, *Open Phys.* 10 (2012) 181–188, <https://doi.org/10.2478/s11534-011-0096-2>.
- [80] M. Vladimirova, M. Stengel, A. De Vita, A. Baldereschi, M. Böhlinger, K. Morgenstern, R. Berndt, W.-D. Schneider, Supramolecular self-assembly and selective step decoration on the Au(111) surface, *Eur. Lett.* 56 (2001) 254, <https://doi.org/10.1209/epl/i2001-00514-3>.
- [81] F. Hanke, J. Björk, Structure and local reactivity of the Au(111) surface reconstruction, *Phys. Rev. B*. 87 (2013) 235422, <https://doi.org/10.1103/PhysRevB.87.235422>.
- [82] W. Xiong, J. Lu, G. Zhang, R. Duan, B. Fu, G. Niu, Y. Yang, L. Gao, L. Chen, J. Cai, Soliton wall and Au adatom-induced trans-to-cis isomerization promoting the formation of multiple pairs of chiral isomers of methylcyano-functionalized molecules, *J. Phys.: Condens. Matter*. 37 (2025) 255402, <https://doi.org/10.1088/1361-648X/addf07>.